# CARBONIZATION

Mitsuhiro Sakawa*1, Katsuhiko Shiraishi*1,
Yasuhiro Aramaki*2 and Toshiaki Okuhara*1
*1 NIPPON STEEL CORP.
*2 NIPPON STEEL CHEMICAL

## 1. Introduction

Research on the mechanism of coal carbonization is indispensable when the production of coke in the oven chamber with higher efficiency is considered. In the past, however, the coal carbonization process has been regarded as a kind of black box and has been estimated from the properties of coal charged and the quality of coke produced. For coal is complex in structure and the oven chamber is a batch unit that is at different temperatures in different portions. Among the other causes are by-products of complex structure that are generated in addition to coke, and expansion, shrinkage and other physical changes that take place with temperature rise.

The measured physical and chemical changes of coal particles are described here. A new apparatus was developed for the in situ observation of the physical changes that the coal particles undergo as mass in the oven chamber during carbonization. This paper also explains a model developed for estimating coke quality from coal properties and carbonization conditions by utilizing these results.

## 2. Pyrolysis Process of Coal Particles

### 2.1 Physical Changes

When coking coal is heated, its characteristic physical phenomena are softening, melting and solidification into semicoke at temperature between 300°C and 500°C. These conditions differ with the type and rank of coal.

The morphological changes of coal particles during heating and the bonding of coal particles by softening and melting were observed under a microscope (Photo. 1).

(Photo. 1)

When heated, coal particles form semicoke through the following stages:

(1) Bubbles form in coal particles.

(2) Bubbles grow, coalesce and grow further.

(3) Coal particles expand.

(4) Coal particles bond together.

(5) Coal particles resolidify into semicoke.

These results of observation indicate that some semicoke retains the contour of coal particles and some does not. The transformation temperatures of coal particles during the heating process are analyzed according to micrographs and sample temperature measurements in Fig.1: temperature at which pores form in vitrinite particles; temperature at which coal particles contact and fuse; and temperature at which vitrinite particles develop anisotropic structure. Figure 1 shows that the temperature at which coal particles contact and fuse and the temperature at which vitrinite particles develop anisotropy vary with the rank of coal.

(Fig. 1)

2.2 chemical changes

The chemical structure of coal is not yet fully clear. It is thus difficult to study the change in the chemical structure of coal in the pyrolysis process. For example, attempts have been long made to estimate the pyrolysis process of coal from the composition of generated gases that can be analyzed. The results of research by an electron spin resonance (ESR) spectrometer with a high-temperature cavity are reported below.

Coal is a complex mixture of organic compounds and when heated, it is converted into coke, which is inorganic carbon. During this heating process, there should be generation and disappearance of unpaired electrons (spins) due to bonding and dissociation of molecules. A high-temperature sample cavity was attached to an ESR spectrometer that measures the spin concentration and the behavior of unpaired electrons was investigated during the carbonization of coal. First, the spin change of compounds containing aromatic rings was investigated as the compound was heated. It was found as a result that when anisotropy develops in

coke formed, the spin concentration markedly increases during the heating process. The measured change in the spin concentration of coal during the heating process is shown in Fig.3. Figure 4 is a plot of the maximum spin concentration of coals of different ranks. When coke anisotropic texture develops, spin concentration during heating process increases. These findings suggest that the development of anisotropic coke structure is mainly promoted by reactions involving the increase in the spin concentration during carbonization.

(Fig. 3)

(Fig. 4)

Next, aluminum chloride ($AlCl_3$) was added to organic compounds containing aromatic rings and the spin change of the organic compounds was investigated during heating. Organic compounds with three or less aromatic rings indicated spin changes different from those of organic compounds with four or more aromatic rings. The spin concentration during the heating process increases with increasing $AlCl_3$ additions when the compound contains three or less aromatic rings (Fig. 5) but decreases with increasing $AlCl_3$ additions when the compound contains four or more aromatic rings (Fig.6). As $AlCl_3$ was added to coals, decrease in the spin concentration during the heating process was observed in coals of every carbonization degree. It is estimated from these results that coal may be composed of four or more aromatic rings. Of course, the effects of functional groups and side chains must be studied as well.

(Fig. 5)

(Fig. 6)

3. In Situ Observation of Coal Carbonization in Oven Chamber

When the carbonization process of coal in the oven chamber is considered, its physical and chemical changes take place simultaneously as shown in Fig.7. As far as the physical changes are concerned, dehydration occurs at 100°C, softening and melting take place in the vicinity of 400°C, followed by solidification and shrinkage. The chemical changes start with evolution of primary tar and gases at approximately the same time as the softening and melting of coal particles. Methane, carbon dioxide and carbon monoxide are initially generated, and the hydrogen content increases with increasing temperature. When these phenomena are considered in the coke oven, there is sometimes created a temperature gradient of 1000°C at the wall and 100°C at the center of the coal charge. As the physical changes, the coke layer is shrunk at the wall while the coal charge is dehydrated at the center. The same is true of the chemical phenomena involved. Few instrumental means were formerly available for investigating coal phenomena in the presence of such a temperature gradient.

(Fig. 7)

3.1 Development of Apparatus for In Situ Observation of Carbonization Process by Computerized Tomographic Scanner

Coal and coke are mainly composed of carbon, hydrogen and oxygen, which are similar to the elemental constituents of the human body. With attention focused on this point, a method was developed whereby the carbonization process of coal can be observed by a soft x-ray computerized tomographic (CT) scanner used in medical examinations.

(Photo. 2)

A general view of the apparatus is shown in Photo. 2. A small coke oven was

set in a medical CT scanner. The technical points considered when developing the small coke oven are as follows:

(1) Selection of material that does not readily absorb x-rays

The coke oven cannot be made of metals and other materials with high x-ray absorption coefficients because they distort CT images.

(2) Construction to keep the temperature outside of the oven in the CT scanner at 25 ± 2°C

The x-ray detector is made of many semiconductors and thus must not be exposed to high temperatures and suddeen temperature changes.

(3) Prevention of waste gas leakage from oven

As the CT scanner must be installed in a lead-lined, airtight room, the leakage of gas and tar from the oven is not allowed.

In view of the above requirements, the oven walls were made of graphite and were heated by high-frequency induction current. The oven was covered with a water-cooled jacket and water, maintained at a constant temperature, was passed through the jacket to keep the oven outside temperature at 25 ± 2°C. The waste gas was cleaned by three filters and washed with water before it was discharged as clean air outside of the room.

### 3.2 Results of Observation

The CT images of coal during the carbonization as observed by the apparatus are shown in Photo. 3. Dark areas indicate high density.

(Photo. 3)

The coal charge is shown to be carbonized as follows. As the oven wall temperature is raised, the resultant evaporation of moisture lowers the apparent bulk density of the coal charge and makes the coal charge appear white on either oven wall (Photo. 3(b)). A further rise in the wall temperature forms a white

plastic layer is very low in bulk density. As the plastic layer moves toward the center, wedge-shaped cracks are formed from the oven wall toward the center (Photo. 3(d)). Cracks are shown to initiate from the oven bottom (Photo. 3(e)). When the plastic layers meet at the center, cracks are formed from the center toward the wall (Photo. 3(g) and (h)). The shrinkage of the entire coke layer is evident together with the propagation of cracks (Photo. 3(g) and (h)).

The results of observation varies with charge coal properties, charging conditions and carbonization conditions in this way. Photo. 4 shows the CT images of Blue Creek coal charges of different bulk densities (maximum fluidity log (DDPM) = 3.27 and volatile matter (VM) = 24.5%.

(Photo. 4)

4. Model for Estimating Coke Quality in Oven Chamber

In the past, coke quality has been estimated from coal properties under constant carbonization conditions. Here is described a model developed to estimate the distribution of coke quality between the oven wall and coal charge center from the input data of coal properties, carbonization conditions and oven conditions.

4.1 Drum Index (DI)

The drum index (DI) of coke was assumed to be a function of the porosity and matrix strength of coke. The estimate of porosity is described first.

The CT scanner described in the previous chapter is also an apparatus for measuring the x-ray absorption coefficient (CT value) on the measured plane. The measured CT values of coal midway in the carbonization process are shown in Photo. 5. With attention attached to the fact that the CT value of a material varies in proportion to the density of the material, a method was developed for converting the CT value into the density. The density distribution of coal as

measured in the carbonization process is shown in Fig.8. The change in the density of the plastic layer as observed by the CT technique is V shaped as evident from Fig.9. If the maximum density ($\rho^c_{max}$) of the resolidified layer in Fig.9 is corrected for shrinkage, the density of coke can be determined. As the resolidified layer gradually moves toward the center of the oven chamber, the above calculation is repeated to obtain the porosity of coke to the center of the oven chamber.

(Photo. 5)

(Fig. 8)

(Fig. 9)

The following procedure was considered for calculating the maximum density ($\rho^c_{max}$) of the resolidified layer.

The mean density ($\rho^c_p$) of the plastic layer can be calculated if the width of the plastic layer and the weight loss in the temperature region concerned are determined. The density ($\rho^c_{coal}$) of the coal layer is taken as the bulk density of the coal charge. The minimum density ($\rho^c_{min}$) of the plastic layer is assumed to be located at its center and to depend on its gas pressure and viscosity. It is known that the gas pressure of the plastic layer can be computed from the total dilatation and bulk density of the coal charge and the heating rate and width of the plastic layer.

Figure 9 thus indicates that the maximum density ($\rho^c_{max}$) of the resolidified layer can be calculated if the mean density ($\rho^c_p$) of the plastic layer, density ($\rho^c_{coal}$) of the coal layer and minimum density ($\rho^c_{min}$) of the plastic layer are known and the minimum density ($\rho^c_{min}$) of the plastic layer is located at the center of the plastic layer.

The composition of the porosity estimation model is shown in Fig.10. The heat transfer model was developed by Nippon Steel. The value of porosity estimated by the model are compared with the measured values of porosity in Fig.11.

(Fig. 10)

(Fig. 11)

The estimate of matrix strength is discussed next. When coal is uniformly charged into an oven chamber, coke produced from the coal charge varies in strength in the width direction of the oven chamber under the influence of differences in the heating rate and maximum ultimate temperature in the width direction of the oven chamber. Factors, such as the heating rate, must be thus considered when estimating the matrix strength of coke in the direction of interest.

Merrick assumed that the strength of coke made from a blend of coals A and B would depend on the strength of the boundary between the particles of the two coals and the strength of the individual coals, as shown in Fig.12. The matrix strength ($P_{AB}$) of coke made from the blend of coals A and B is thus given by

$$P_{AB} = X^2 \cdot P_A + 2XY \cdot BS(AB) + Y^2 \cdot P_B \qquad (1)$$

where $P_A$ is the matrix strength of coke made from coal A, $P_B$ is the matrix strength of coke made from coal B, X is the proportion of coal A in the blend, Y is the proportion of coal B in the blend, and BS(AB) is the bond strength between coals A and B.

(Fig. 12)

Merrick measured the strengths ($P_A$, $P_B$) of individual coals A and B and the

strength ($P_{AB}$) of the blend of the two coals, and calculated the bond strength (BS(AB)) between the coals. The present authors decided to estimate $P_A$, $P_B$ and BS(AB) from the properties and carbonization conditions of the coal charge.

To investigate the boundary between coke made from one kind of coal and coke made from another kind of coal, two kinds of coal were charged and carbonized in an electric coke oven so that a coke boundary could be produced from them. Coke boundaries between two different kinds of coal were polished and observed under a microscope. When the results of microscopic observation are plotted with fluidity along the vertical axis and solidification temperature difference along the horizontal axis, a region with good strength is schematically drawn as shown in Fig.13. It was deemed necessary to consider the fludity and rank of coal (represented here by the solidification temperature that is assumed to be proportional to the rank of coal) as other factors that govern the strength of coke. Therefore, the bond strength between two kinds of coal is regarded as a function of fluidity, solidification temperature and solidification temperature difference and is expressed by

$$BS(AB) - F(MF_{AB}, ST, \quad ST) \qquad (2)$$

where $MA_{AB}$ is the mean fluidity of coals A and B, ST is the mean solidification temperature of the two coals, and ST is the solidification temperature difference between them.

(Fig. 13)

Similarly, the matrix strength of coke made from a single kind of coal can be calculated by Eq.(2) if the term ST is made zero. Since a temperature gradient is created across the width of the oven chamber and the fluidity and solidification temperature of the coal vary with the heating rate, the solidification temperature difference is also a function of the heating rate. In other words, the matrix strength computed by Eq.(2) should differ in the width direction of the oven

chamber. To define the actual functional form of Eq.(2), seven kinds of coal were selected from among those actually used in commercial coke manufacture and 21 blends of two kinds of coal each were carbonized in the electric oven mentioned above. A disk-shaped specimen was taken from each of the specified positions in the oven chamber and was tested for matrix strength by a conventional procedure. The temperature gradient at the sampling positions was obtained by blank test, and the fluidity and solidification temperature of the specimens taken from the respective sampling positions were calculated.

If the temperature distribution in the oven chamber is computed by the heat transfer model as described above, the matrix strength of coke taken at each of the sampling positions can be determined from the properties of coal.

As it is known that the drum index (DI) of coke is a function of porosity and matrix strength, the drum index of coke sampled at different positions in the oven chamber can be calculated as discussed above.

### 4.2 Coke Strength after Reaction with $CO_2$ (CSR)

The coke strength after reaction with $CO_2$ (CSR) can be obtained from the drum index (DI) and coke reaction index (CRI). The DI can be calculated as noted in the previous section. The CRI is divided into one term ($CRI_T$) that depends on temperature and another term ($CRI_O$) that does not depend on temperature and is considered to be computable from the properties of coal (vitrinite reflectance, total inerts and alkaline content of ash) as discussed at another panel "Selection of Blends for Cokemaking."

The effects of the following factors were considered for the term $CRI_T$:

(1) The degree of graphitization ($L_C$) determined by Nishioka et al., using the x-ray diffraction technique was employed as a term dependent on the arrangement (graphitization) of carbon.

(2) Considering the change in the structure of coke with heating rate, a term that linearly varies with the heating rate was devised. The effect of this

term is small, however.

(3) The effect of precipitated carbon was assumed to be proportional to the evolved gas and was expressed as a function of the amount, bulk density and volatile matter of the coal charge.

The composition of the model for estimating the DI and CSR of coke is illustrated in Fig.14. The values of DI and CSR estimated by the model are compared with the measured values of DI and CSR in Fig.15. The model was found to be capable of estimating the actual DI and CSR of coke with high accuracy.

(Fig. 14)

(Fig. 15)

## 5. Conclusions

It was dynamically observed for the first time how the physical changes of coal particles during the heating process would differ from those of coal particles when they behave as mass in the chamber of the coke oven. Based on the change in the density distribution of the plastic layer, a coke quality estimation model was developed that can also determine the changes the coal particles undergo in the width direction of the oven chamber.

Although not discussed here, it is necessary to take into account not only physical changes but also chemical changes when estimating the quality of by-products. The quality estimation of by-products will be discussed mainly from the standpoint of chemical changes on the next occasion.

References

1) S.Ida, T.Okuhara and T.Yamaguchi: Proceedings of 54th Special Coke Meeting (1973).

2) M. Sakawa, T. Uno and Y. Hara: Fuel, 62 (1983), p.585.

3) M. Sakawa, T. Uno and Y. Hara: Fuel, 62 (1983), p.571.

4) M.Sakawa, K.Shiraishi, Y.Sakurai and Y.Shimomura: Journal of the Fuel Society of Japan, 66 (1987), p.259.

5) M.Sakawa, K.Shiraishi, Y.Sakurai and Y.Shimomura: Tetsu-to-Hagane, 72 (1986), p.S30.

6) K.Shiraishi, Y.Sakurai, M.Sakawa and Y.Shimomura: Tetsu-to-Hagane, 72 (1986), p.S31.

7) K.Shiraishi, Y.Sakurai, M.Sakawa and Y.Shimomura: Proceeedings of 80th Special Coke Meeting (1986).

8) Y.Aramaki, Y.Miura, Y.Sakurai and M.Sakawa: Tetsu-to-Hagane, 71 (1985), p.S16

9) Y.Aramaki, Y.Miura, Y.Sakurai and M.Sakawa: Tetsu-to-Hagane, 71 (1985), p.S17.

10) K. Tanaka, S. Kamio, Y. Nakagawa and Y. Shinohara: Tetsu-to-Hagane, 71 (1985), p.S1.

11) D. Merrick: Fuel, 62 (1983), p.540.

12) K. Nishioka and S. Yoshida: Tetsu-to-Hagane, 70 (1984), p.343.

Ohnoura coal (contact bond type)

(1) 385℃

small bubbles are exinite durite and Central portion is vitrinite portion formed in homogeneous

↓

(2) 400℃

Bubbles, which are produced in vitrinite or exinite durite, gradually grow

↓

(3) 450℃

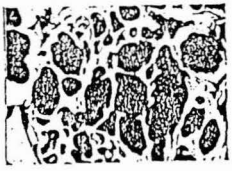

Bubbles in vitrinite are grown and coal portion is thinned. Particle contour is retained. Small particles in surrounding region remain unchanged

↓

(4) 480℃

Solidification temperature is exceeded and semicoke is produced, but contour of coal particles is retained. Small particles at upper right are free from bubbles and converted into semicoke

Std. Douglas coal (flow bond type)

(1) 390℃

Bubbles are formed in vitrinite particles but not in particles of small size

↓

(2) 406℃

Bubbles rapidly grow and particles are spherical and fused with each other

↓

(3) 446℃

Plastic coal is converted into thin film and flows carrying inerts on surface

↓

(4) 520℃

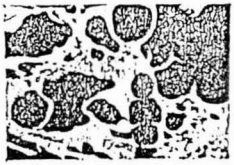

Films of plastic coa meet again and form thick coke wall

Photo. 1. Pyrolysis process of coal particles.

Table 1. Bond types observed during heating process of coal particles.

| Major classification | | Minor classification | Description of bond type | Coal belonging to bond type concerned |
|---|---|---|---|---|
| A | Contact bond | A−1 | Coal particles are resolidified with contour retained, and coke is thick in wall structure and exhibits optical anisotropy | Itmann<br>Balmer |
| | | A−2 | Coal particles are resolidified with contour retained, and coke is thin in wall structure and exhibits no optical anisotropy | Ohnoura<br>Newdell |
| B | Flow bond | B−1 | Coal particles are rich in reactives, show marked flow phenomenon, and when coal particles are resolidified, these components meet and fuse to form thick wall | Std. Douglas<br>Takashima |
| | | B−2 | Coal particles are rich in inerts and molten reactives envelop inerts to form thick wall | Coal Cliff<br>Kuznetsk KJ-14<br>Moura |

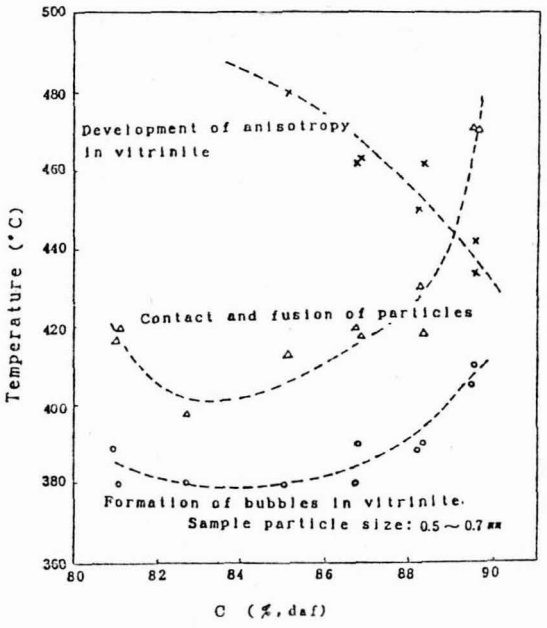


Fig. 1. Relationship between transformation temperature and rank of coal particles during heating process.

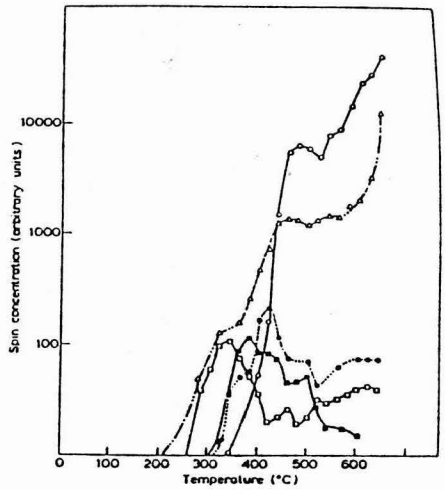


Fig. 2. Spin changes of organic compounds during carbonization. ○, Naphthacene; △, benzopyrene; ●, pyrene; ■, chrysene; □, anthracene

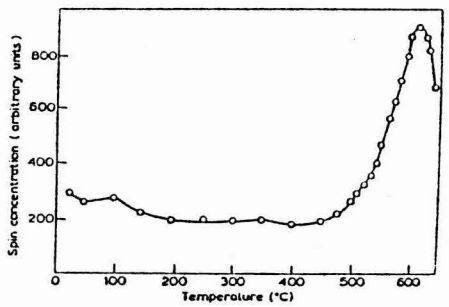


Fig. 3. Spin change of Lancashire coal during carbonization.

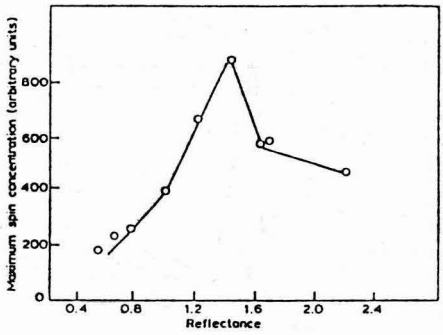


Fig. 4. Variation in maximum spin concentration with vitrinite reflectance during carbonization.

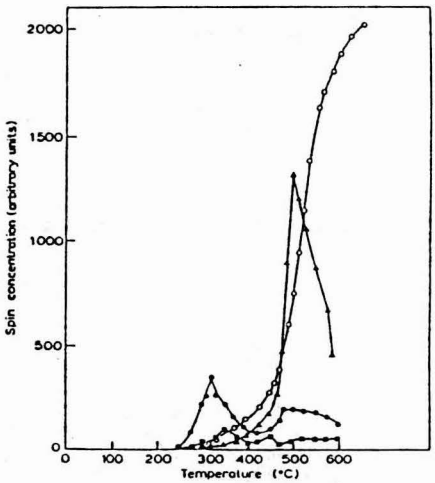


Fig. 5. Spin changes of anthracene (20 mg) during carbonization with $AlCl_3$. ○, 10 mg; ▲, 7.5 mg; ●, 5 mg; ■, 0 mg $AlCl_3$

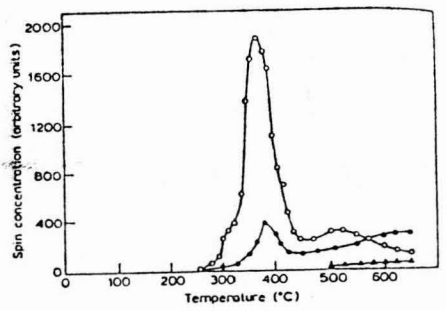


Fig. 6. Spin changes of pyrene (20 mg) during carbonization with $AlCl_3$. O, 0 mg; ●, 5 mg; ▲, 10 mg $AlCl_3$

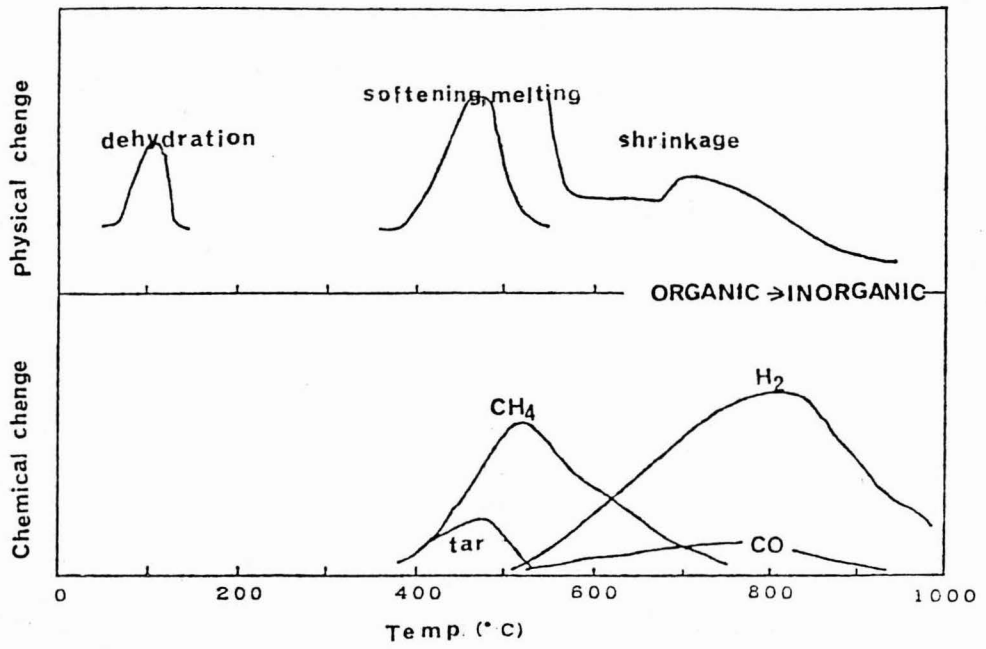


Fig. 7. Pyrolysis behavior of coal.

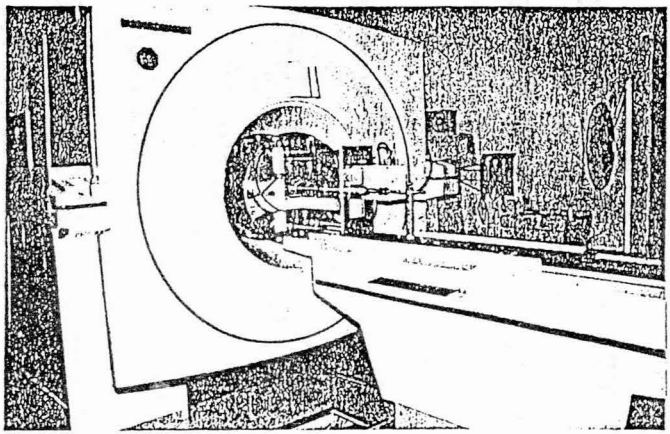

Photo. 2. Apparatus for in situ observation of coal carbonization process using CT scanner.

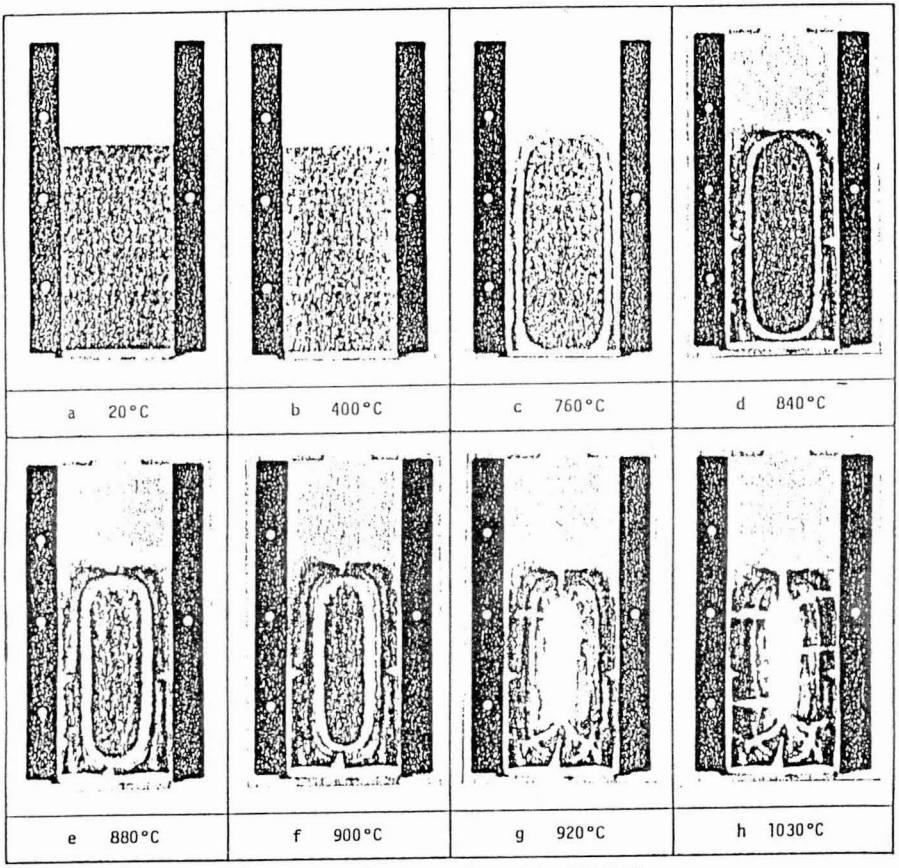


Temperature is measured at the oven wall.

Photo. 3. CT images of coal during carbonization process (volatile matter = 21.6, bulk density = 0.75 t/m$^3$).

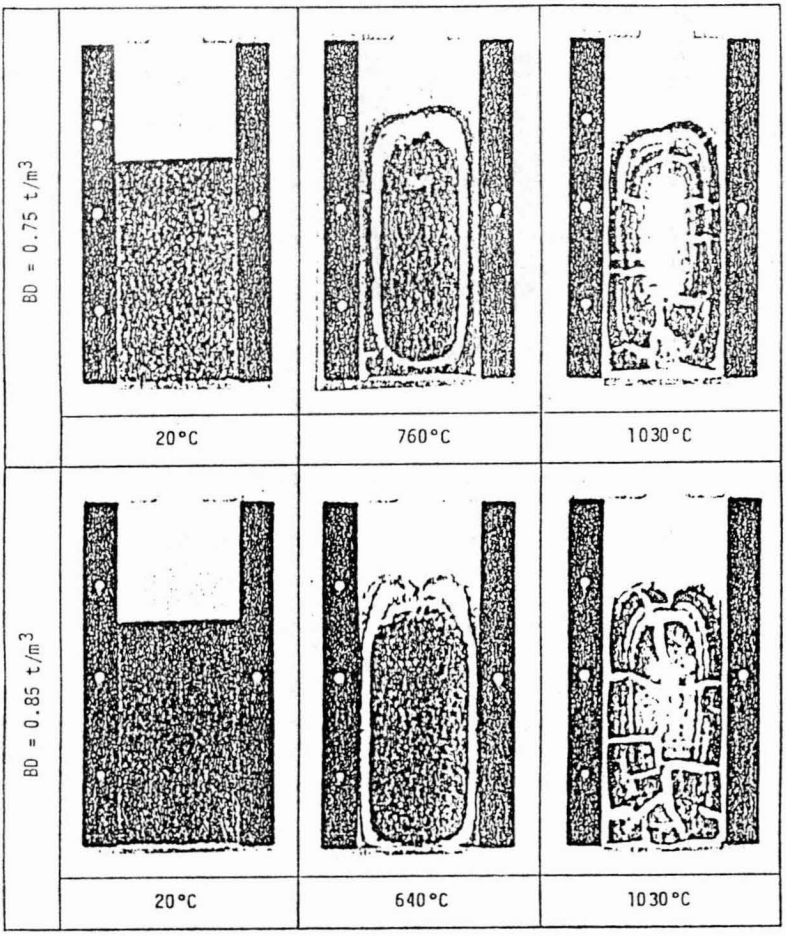


Temperature is measured at the oven wall.

Photo. 4. Comparison of Blue Creek coal charges of different bulk densities in progress of carbonization (volatile matter = 24.5%).

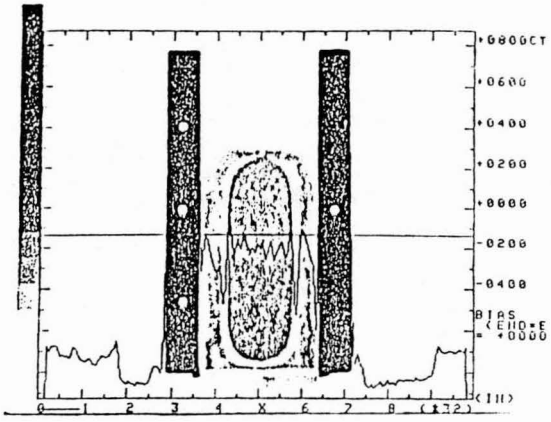


Photo. 5. CT value distribution of coal during carbonization.

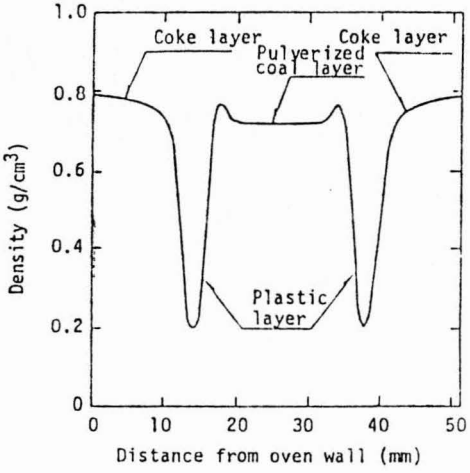


Fig. 8. Change in density distribution during carbonization.

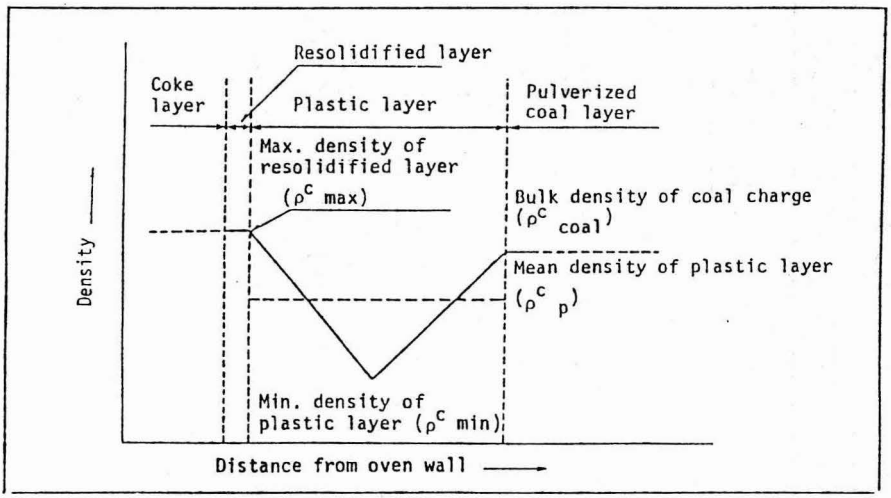


Fig. 9. Density distribution of plastic layer.

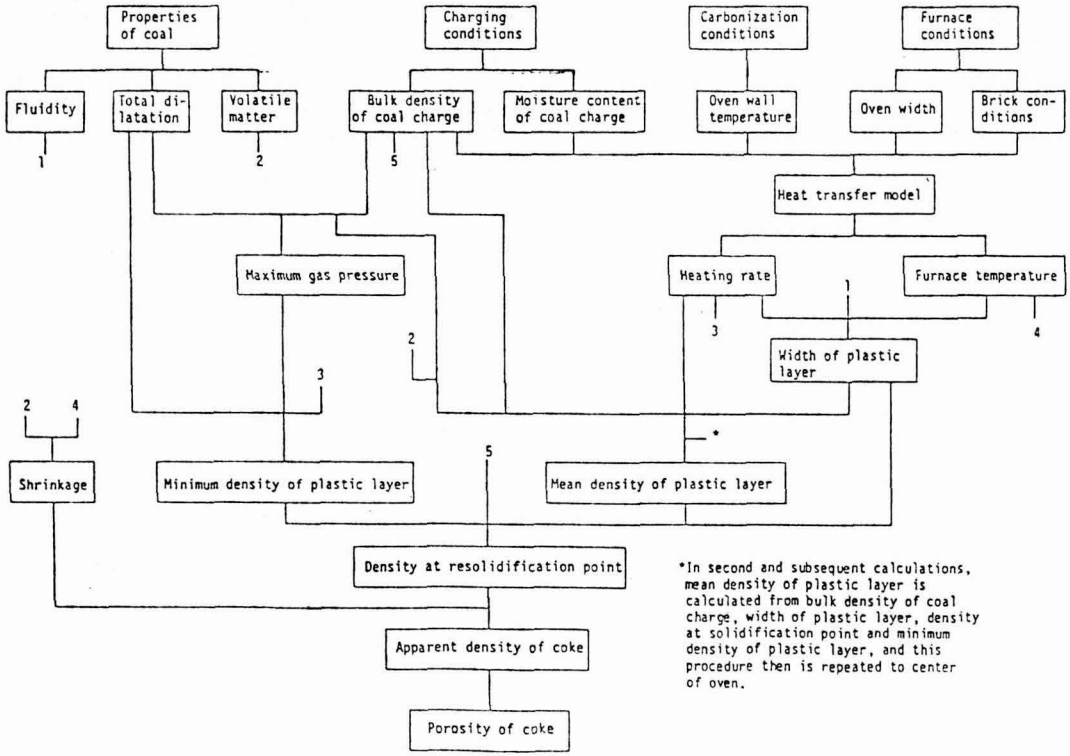


Fig. 10. Composition of coke porosity estimation model.

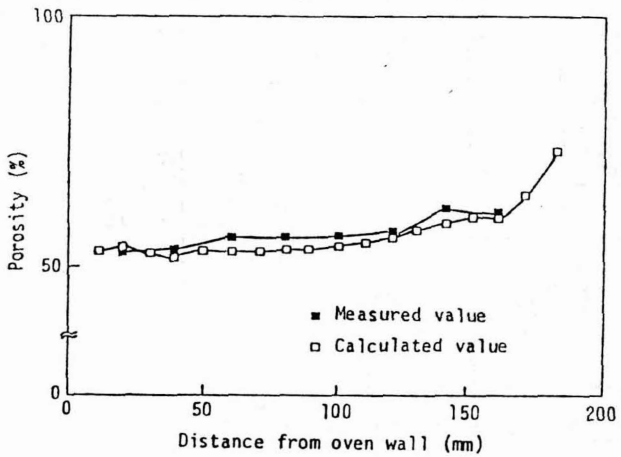


Fig. 11. Estimate of coke porosity.

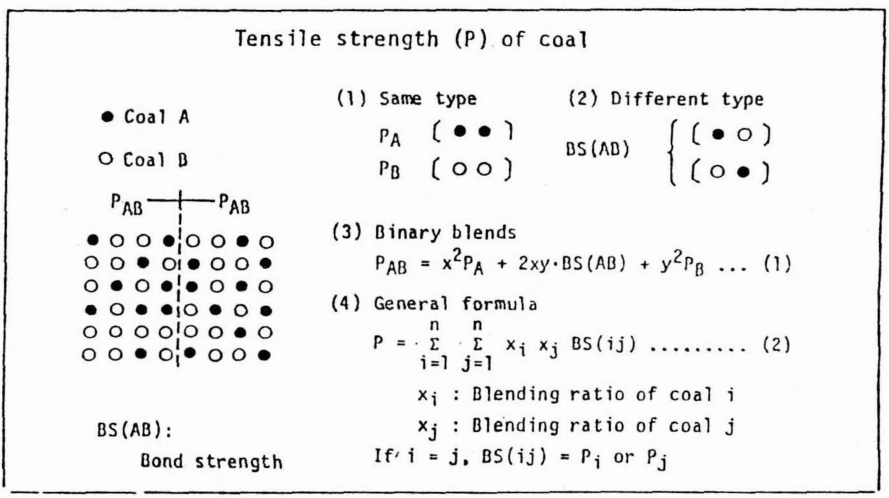


Fig. 12. Concept of estimation of matrix strength of coke.

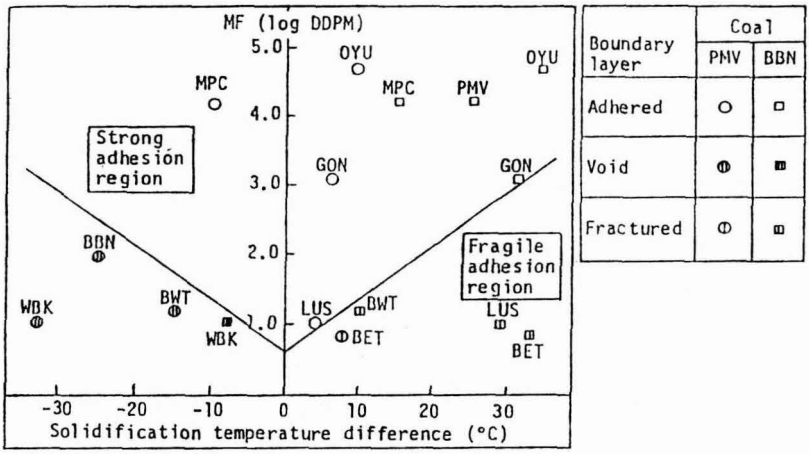


Fig. 13. Adhesion of coke from standpoint of solidification temperature difference and fluidity of coal.

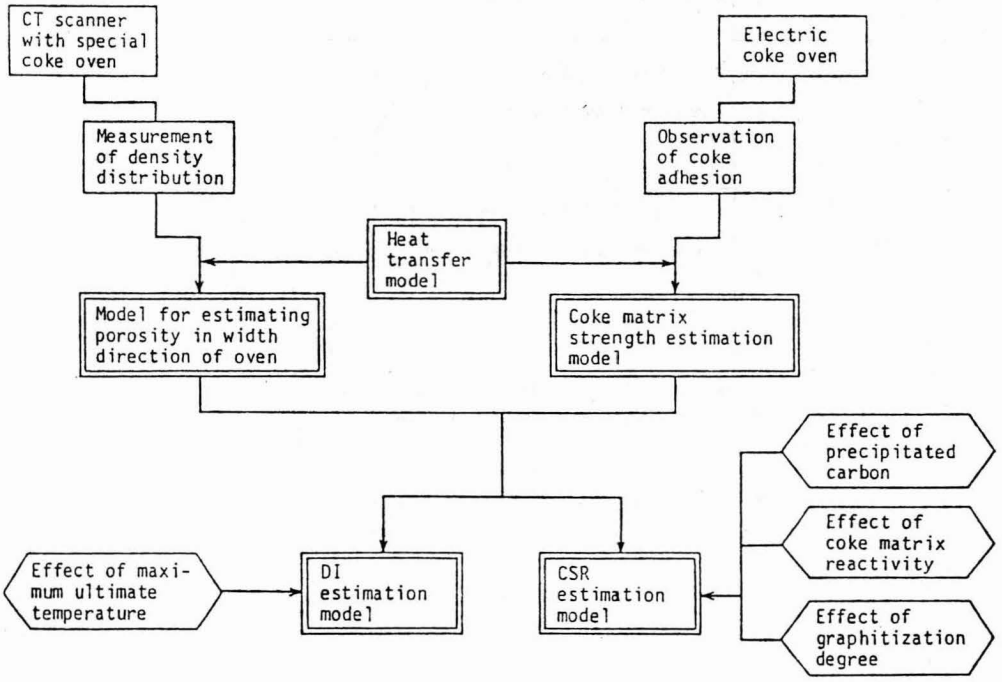


Fig. 14. Composition of DI and CSR estimation model.

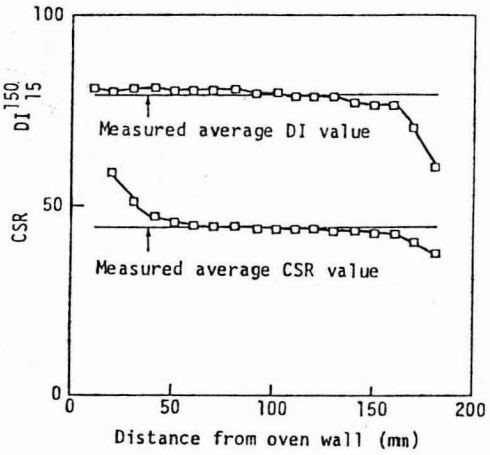


Fig. 15. Estimate of DI and CSR.